

TOP-LEVEL AIRCRAFT REQUIREMENT TRADE STUDIES FOR HYDROGEN FUEL CELL REGIONAL AIRCRAFT

Mario Di Stasio[1], Fabrizio Nicolosi[1]

[1]University of Naples Federico II (UNINA), Department of Industrial Engineering, DAF research group

Abstract

This paper investigates the influence of top-level aircraft requirements on the conceptual design of hydrogen fuel cell-powered regional aircraft. Three representative requirement sets are analysed, ranging from a demanding reference case to requirements closer to current regional turboprop operations. For each set and selected variants, optimized hydrogen-powered configurations are compared with conventional turboprop counterparts in terms of sizing, installed power, mass, block energy, and direct operating costs. The results show that hydrogen fuel cell aircraft are highly sensitive to payload, cruise, field performance, and wing span requirements. The most demanding requirement set preserves the highest operational capability but leads to the largest mass and specific block energy penalties. Conversely, less demanding requirements improve energy performance per seat and nautical mile, but reduce operational flexibility. An intermediate requirement set provides the most balanced compromise, limiting energy penalties and improving DOC competitiveness under baseline fuel cost assumptions.

Keywords: conceptual design, hydrogen, electric propulsion, decarbonization

1. Context and objectives

In recent years, the need for substantial actions aimed at mitigating the environmental impact of human activities, particularly in relation to climate change, has gained increasing attention, not only within the scientific community but also among policymakers and the general public. In response, international institutions and national governments have initiated a wide range of measures to reduce anthropogenic emissions and to foster the development of more sustainable technologies. These efforts have translated into the funding of numerous research programs intended to deliver concrete solutions over the short, medium, and long term.

Within this broader framework, aviation, and commercial aviation in particular, has also been called upon to undertake decisive actions to reduce its environmental footprint. Although aviation is not currently the dominant contributor to global CO_2 emissions among transportation modes, its relevance is strongly amplified by the sustained growth in air traffic observed over recent decades, especially driven by emerging economies. While incremental reductions in fuel burn and emissions can be achieved through improvements in aerodynamic efficiency, structural mass optimization, and propulsion system performance, the ambitious targets set for medium- and long-term decarbonization scenarios largely require a profound rethinking of aircraft powerplants and the adoption of alternative energy carriers to conventional kerosene.

In this context, hydrogen-powered aviation has progressively emerged as a promising pathway toward zero-carbon operations at the mission level, with fuel cell-based electric propulsion systems often proposed as a potential replacement for thermal engines. Although the regional aircraft segment does not represent the largest share of overall commercial aviation emissions, it has attracted considerable interest and is frequently identified as one of the most suitable entry points for the introduction, validation, and early commercialization of disruptive propulsion technologies. This is primarily due to the typical characteristics of regional operations, namely passenger capacities up to approximately 100 seats and stage lengths generally below 1,000 km. These features facilitate the integration of novel energy storage solutions, such as cryogenic hydrogen

tanks, as well as new propulsion-related subsystems, including fuel cell stacks and their associated thermal management and air supply systems. Importantly, such integration can often be achieved without resorting to radically unconventional aircraft configurations (such as double fuselages, non-circular fuselage cross-sections, or hybrid wing-body layouts) thus preserving the conventional tube-and-wing architecture. At the same time, the combination of projected gravimetric power densities, expected system masses, and moderate power demand levels makes the regional aircraft class particularly suitable for a technically feasible implementation of fuel cell-based propulsion.

Recent studies have investigated hydrogen fuel cell propulsion for small, regional, and short-range aircraft using conceptual design and optimization methods, often highlighting the strong coupling between aircraft sizing, fuel cell system performance, hydrogen storage, balance-of-plant components, and mission requirements. Nicolay et al. [1] performed a clean sheet design and multidisciplinary optimization of a general aviation aircraft using liquid hydrogen and fuel cells, extending the SUAVE framework to include hydrogen energy networks and fuel cell-based propulsion modelling. Svensson et al. [2] implemented methods for sizing and mission assessment of regional hydrogen fuel cell aircraft also in SUAVE, including fuel cell propulsion, liquid hydrogen storage, airframe resizing, tank thermodynamics, and mission performance effects, with application to ATR-like regional aircraft. At subsystem level, Massaro et al. [3] and Schröder et al. [4] developed integrated sizing and optimization approaches for proton exchange membrane (PEM) fuel cell systems for regional aircraft propulsion, showing the strong coupling between stack performance, balance-of-plant components, thermal management, mass, efficiency, drag, and volume. Quaium et al. [5] focused specifically on the cooling system of a hydrogen-powered regional concept aircraft, comparing one-phase and two-phase cooling architectures and highlighting the aircraft-level relevance of cooling system mass, drag, and auxiliary power demand. Extending the analysis toward larger transport class applications, Ahluwalia et al. [6] assessed a PEM fuel cell-powered single-aisle regional aircraft representative of the Airbus A220-100 class, coupling aircraft sizing, electric propulsion, heat rejection, fuel cell degradation, duty-cycle performance, and economic analysis to identify the main technology gaps for hydrogen fuel cell aircraft.

Within this framework, a key research question arises concerning the identification of the most favourable set of top-level aircraft requirements (TLARs) for fuel cell-powered regional aircraft. Unlike conventional designs, hydrogen and fuel cell architectures introduce strong couplings between performance requirements, energy storage integration, system mass, and overall aircraft efficiency. TLARs such as cruise speed, design range, climb performance, field length constraints, and payload capability directly influence not only the aerodynamic and structural sizing of the aircraft, but also the installed fuel cell power, the size and placement of hydrogen tanks, and the characteristics of auxiliary systems. As a result, TLARs that are well suited for kerosene-based aircraft may lead to suboptimal or even prohibitive solutions when applied unchanged to fuel cell configurations, in terms of total energy demand and direct operating costs (DOC).

Consequently, this work focuses on two closely related objectives. First, it aims at identifying combinations of TLARs that are particularly favourable for the integration of fuel cell-based propulsion systems in regional aircraft, while limiting the penalties in energy consumption and operating costs relative to contemporary conventional counterparts. Second, it investigates the sensitivity of the aircraft design to variations in selected TLARs, with the goal of quantifying how changes in ground, climb, cruise, and operational requirements propagate through the design process and affect the final aircraft configuration. In this way, this analysis will provide insight into the robustness of fuel cell-powered regional aircraft concepts and supports the definition of requirement sets that are better aligned with the intrinsic characteristics of hydrogen-electric propulsion.

The studies presented in this paper are conducted within the framework of the Clean Aviation FAME project (*Fuel cell propulsion system for Aircraft Megawatt Engines*) coordinated by Airbus. FAME aims to support the development of a compact, lightweight, and high-efficiency hydrogen fuel cell electric propulsion system for short-range aviation. The targeted powertrain is based on an aviation-native fuel cell system supplied by liquid hydrogen and designed to deliver multi-megawatt power levels, in the range of approximately 2–4 MW, while accounting for the integration of the main propulsion-related subsystems, including nacelles, propellers, thermal management, and auxiliary

equipment. Within this project framework, the activities presented in this paper contribute to Work Package 2, which focuses on aircraft conceptual design and on the assessment of propulsion-system integration effects at aircraft level. The reference FAME aircraft concept is a short-range, propeller-driven platform, representative of a 2040 entry-into-service (EIS) scenario and based on liquid hydrogen fuel cell propulsion. The baseline configuration considered within the project features four fuel cell propulsion units and adopts a conventional tube-and-wing layout.

2. Implementation

2.1 Definition of requirements

From an operational standpoint, the design exercise carried out in this work is driven by the three sets of top-level aircraft requirements reported in Table 1. These sets are intended as representative baseline scenarios rather than isolated point-design specifications, and they provide the starting conditions for the subsequent sensitivity analyses. In particular, variations are applied to selected requirements associated with ground performance and cruise performance, with the aim of assessing how changes in operational constraints propagate through the aircraft sizing process and affect the resulting hydrogen fuel cell aircraft concepts. The first requirement set, referred to as TLARs-1, is closely aligned with the reference assumptions adopted within the FAME project. At the opposite end of the investigated range, TLARs-3 is defined to be broadly representative of current regional turboprop operations, taking the ATR 72-600 as a reference while introducing limited deviations from its actual characteristics and performance levels. Finally, TLARs-2 provides an intermediate scenario between these two cases, allowing the analysis to explore a gradual transition from a FAME-oriented reference aircraft toward requirements closer to those of an existing in-service regional platform.

Table 1 – Sets of top-level aircraft requirements adopted for the conceptual design of conventional and fuel cell electric aircraft.

	Sets of requirements		
Requirements	**TLARs-1**	**TLARs-2**	**TLARs-3**
Design range	1,000 nm	1,000 nm	800
Design payload	100 PAX @95 kg	90 PAX @95 kg	80 PAX @95 kg
Initial cruise altitude capability	27,000 ft	25,000 ft	20,000 ft
Cruise Mach number	0.55	0.50	0.45
Take-off field length (TOFL)	1,400	1,400	1,300
Landing field length (LFL)	1,400	1,400	1,300
Approach category *	C	B	B
ICAO airport code **	C	C	C
Reserves	100-nm alternate, 30-min holding, 5% contingency fuel		
LH2 tank dormancy requirement ***	240 min @ ISA+40°C w/o venting		

* B (91 < approach CAS < 120 kn), C (121 < approach CAS < 140 kn).
** C (24 < wing span < 36).
*** Only applicable to fuel cell engine designs.

For each of the three baseline requirement sets introduced in Table 1, both hydrogen fuel cell-powered and conventional turboprop aircraft are designed and assessed. The objective of this parallel sizing process is not to compare two aircraft sharing the same propulsion technology maturity horizon, but rather to quantify the implications of introducing hydrogen fuel cell propulsion with respect to a conventional reference representative of current regional-aircraft technology. In this sense, the conventional configurations are used as benchmark aircraft against which the mass, performance, energy consumption, and operating characteristics of the hydrogen-powered concepts can be evaluated.

The two families of aircraft are therefore driven by the same operational requirements, but they are not based on the same EIS assumptions. Hydrogen fuel cell-powered configurations are sized

assuming a 2040 EIS, consistently with the mid/long-term technological horizon generally associated with the maturation of aviation-grade fuel cell systems, cryogenic hydrogen storage, electric propulsion components, and the related onboard subsystems. Conversely, the conventional turboprop configurations are modelled assuming a 2020 technology level, broadly representative of the ATR 72-600 and of currently available regional turboprop aircraft. As a result, the conventional aircraft designed around TLARs-1 to TLARs-3 can be interpreted as ATR 72-like reference aircraft scaled to different payload, range, and performance requirements, including more demanding operational constraints where applicable.

This choice is also reflected in the propulsion system assumptions adopted for the conventional aircraft. In particular, the engine specific fuel consumption (SFC) is defined starting from values representative of PW127-class turboprop engines, with available shaft power levels close to those installed on the ATR 72-600, and only limited corrections are introduced to account for size-related effects when different power ratings are required by the aircraft sizing process. In this way, the conventional aircraft retain the technological characteristics of current in-service regional turboprops, rather than representing a speculative future clean sheet kerosene-powered aircraft.

The rationale behind this approach is consistent with the type of comparison typically adopted in European research activities addressing disruptive aircraft technologies. Hydrogen-powered concepts targeting a 2035–2040 EIS are commonly assessed against current comparable conventional aircraft, designed or resized to satisfy similar requirements. This provides a meaningful benchmark for evaluating whether the additional complexity, mass, and integration challenges associated with fuel cell propulsion and liquid hydrogen storage can be justified by the expected environmental and operational benefits. Moreover, it avoids introducing assumptions on hypothetical future conventional turboprop aircraft and engines that may not be representative of realistic industrial development pathways, especially in a scenario where hydrogen technologies and the corresponding infrastructure are assumed to have reached sufficient maturity.

Although the propulsion technologies and EIS assumptions differ, the overall aircraft architectural layout is intentionally kept as consistent as possible across the investigated configurations. All concepts adopt a conventional propeller-driven aircraft arrangement, featuring a high-wing configuration, T-tail, under-wing propulsor installation, and fuselage-mounted landing gear. In addition, both the hydrogen-powered and conventional kerosene-fuelled aircraft are designed with the same cabin arrangement, based on a five-abreast layout in a 2+3 configuration, for all three requirement sets. For the hydrogen-powered aircraft, liquid hydrogen storage is accommodated through two tandem cryogenic tanks installed in the rear fuselage section, downstream of the pressure bulkhead, while the cabin length is adapted to the passenger capacity associated with each requirement set. Across all hydrogen-powered configurations, the tanks are sized by adopting the same dormancy requirement, corresponding to 240 minutes at ISA+40 °C without venting.

2.2 Methodology

The analyses presented in this work are performed using JPAD [7][8][9], a modular framework for aircraft conceptual and preliminary design developed at the University of Naples Federico II by the DAF (*Design of Aircraft and Flight technologies*) research group, in collaboration with SmartUp Engineering. JPAD builds on the broader experience gained by the DAF research group in collaborative aircraft multidisciplinary conceptual design and optimization, including previous AGILE/AGILE 4.0 activities [10][11][12]. It is based on an object-oriented architecture implemented in Java and provides a comprehensive environment for the multidisciplinary assessment of aircraft configurations. The framework enables the detailed parameterization of conventional and unconventional aircraft and supports the evaluation of mass properties, centre-of-gravity position, aerodynamic characteristics, flight performance, environmental indicators, and direct operating costs.

JPAD combines semi-empirical methods available in the literature with in-house models developed for aircraft-level design studies. Within the framework, flight performance is evaluated through simulation-based routines, including time-marching approaches and, when required, the solution of systems of ordinary differential equations. Over recent years, the framework has been extended to support the modelling of advanced propulsion architectures, with particular attention to hybrid-

electric and full-electric configurations, including hydrogen fuel cell-powered aircraft.

For the present study, JPAD represents the central environment of the aircraft sizing and optimization process. The adopted workflow enables the parametric variation and optimization of the main aircraft design variables, including wing planform characteristics and installed shaft power, with the objective of minimizing mission block fuel/energy consumption, while satisfying the imposed top-level aircraft requirements [13]. The overall process is depicted in Figure 1 and starts from the definition of a baseline aircraft configuration and a set of technology-level assumptions. The aircraft geometry is then updated according to the selected design variables and derived quantities, including wing area, wing aspect ratio (AR), wing span, fuselage dimensions, nacelle geometry, tailplane layout, propulsion-system installation, and onboard systems positioning.

The resulting configuration is analysed through coupled iterative convergence loops. A first loop ensures consistency among mission requirements, fuel/energy consumption, and maximum take-off mass. For hydrogen-powered configurations, a second loop addresses the integration of the liquid hydrogen storage system, verifying the compatibility between the required hydrogen mass, the available tank volume, and the imposed installation constraints. When needed, the aircraft geometry is updated accordingly, so that the final configuration remains consistent with both mission energy demand and hydrogen storage integration requirements. Once convergence is achieved, JPAD performs a complete performance analysis, including take-off, climb, cruise, descent, landing, payload-range evaluation, and optional off-design or alternative mission assessments.

A key feature of the workflow is the modular representation of the propulsion system. In JPAD, the powerplant architecture is defined through component-based input data, allowing the main elements of the propulsion chain to be modelled separately and then integrated at aircraft-level. For fuel cell-powered configurations, this includes fuel cell stacks, electric machines, power electronics, gearboxes, propellers, and auxiliary systems. The behaviour of the fuel cell and electric propulsion system is represented through a bottom-up approach, in which component-level characteristics are propagated to system-level quantities such as efficiency, output power, mass, and volume. This modular structure facilitates the integration of updated assumptions coming from parallel technology-development activities.

For hydrogen-powered aircraft, JPAD is coupled with dedicated in-house tools that model subsystems not required for conventional turboprop configurations. The sizing of the cryogenic hydrogen tanks is performed using a MATLAB-based tool derived from the methodology proposed by Winnefeld et al. [14]. The tool estimates tank geometry, structural and insulation masses, and overall storage-system characteristics as a function of the required hydrogen quantity, mission profile, dormancy requirements, and installation constraints, such as the maximum allowable tank diameter. To support aircraft-level design loops and parametric studies, detailed tank-sizing results can also be condensed into surrogate models, enabling rapid evaluation of hydrogen storage characteristics during iterative aircraft sizing and optimization.

The integration of the fuel cell thermal management system is supported by a dedicated MATLAB-based physics-driven tool for the analysis of air intakes and cooling ducts integrating heat exchangers [15]. The tool performs both design-point and off-design analyses of the intake system, including diffuser, heat exchanger, transition ducting, and ducted cooling fan. Heat exchanger sizing is based on the ε-NTU method, while pressure losses, curvature effects, and duct-related losses are evaluated through geometry-dependent models. The tool provides estimates of the main cooling-system performance quantities and associated drag contributions, including momentum drag, heat exchanger-related losses, and external cowling drag. For integration within the aircraft design loop, representations of these effects are used to account for the aircraft-level penalties associated with fuel cell thermal management.

DOC predictions are based on the calculation approach described in [16][17], which enables the inclusion of cost contributions associated with disruptive propulsion system architectures in both capital and operational expenditures.

The converged aircraft designs are finally used to generate response surfaces and design space representations. These response surfaces allow the feasible design space to be identified for each set of top-level aircraft requirements and for each propulsion architecture. Optimization studies are

then performed by selecting the configurations that satisfy all imposed constraints while minimizing the chosen objective function, such as design mission block energy or block fuel, and/or direct operating cost.

An analogous workflow is adopted for conventional turboprop aircraft, although in this case the additional convergence loop associated with hydrogen tank sizing, storage volume compatibility, and fuselage length update is not required.

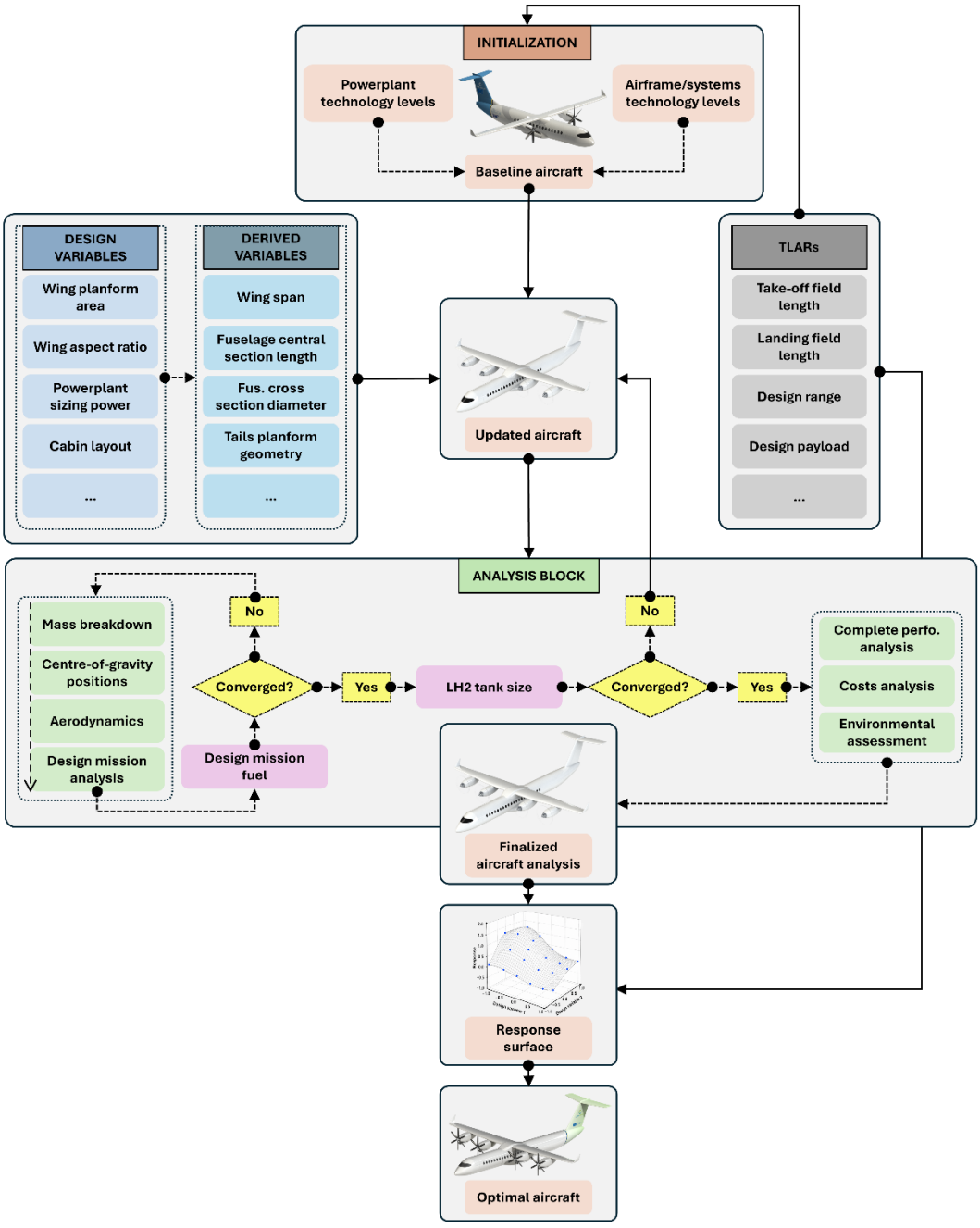


Figure 1 – Schematic representation of the conceptual design workflow implemented by JPAD for hydrogen-powered aircraft with fuel cells.

2.3 Assumptions

2.3.1 Level-of-technology-related assumptions

The hydrogen-powered aircraft variants considered in this work adopt a fuel cell electric propulsion architecture, schematically represented in Figure 2. Liquid hydrogen is stored onboard in cryogenic tanks installed in the rear fuselage and is supplied to a set of fuel cell systems integrated within wing-mounted nacelles. Each fuel cell system is composed of several fuel cell stacks operating in parallel, allowing the required power level to be achieved while preserving modularity and redundancy at

propulsion system level.

The fuel cell systems are supported by two main auxiliary subsystems. The first one is the air supply line, which provides the oxygen required for the electrochemical reaction and includes the compression system needed to ensure adequate operating conditions across the flight envelope, particularly at altitude. The second one is the cooling line, which is responsible for rejecting the waste heat generated by the fuel cells and includes the heat exchangers and related ducting required for thermal management. Each fuel cell system is therefore treated as an integrated power generation unit, including the stacks and the ancillary components required for air supply, cooling, and operation. The electrical power produced by the fuel cells is then delivered to the propeller through the power line, composed of the electric motor, power electronics, cabling, and reduction gearbox.

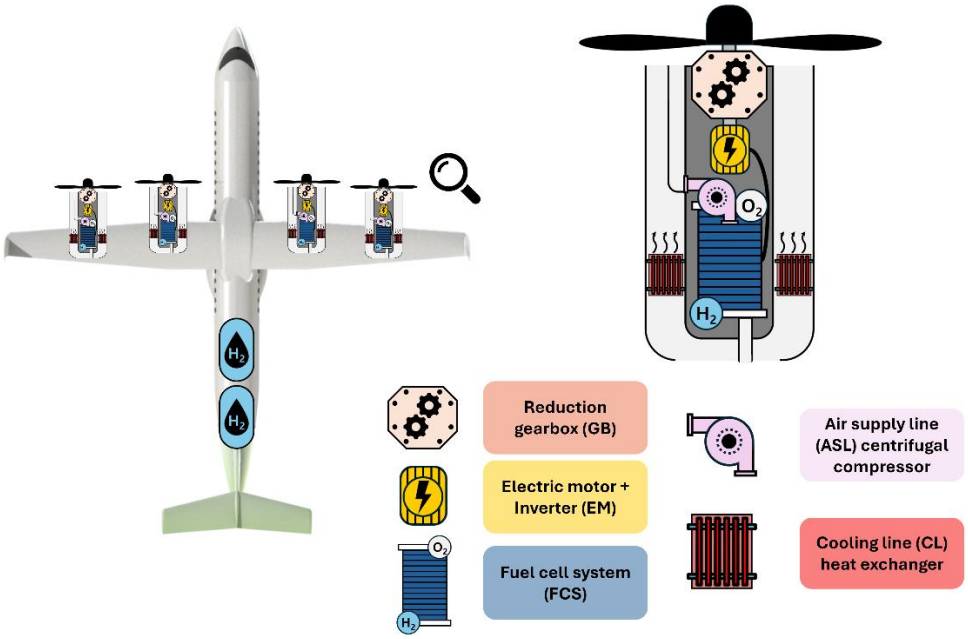


Figure 2 – Schematic representation of the hydrogen fuel cell powerplant architecture adopted for the aircraft variants analysed in this study, including rear-fuselage liquid hydrogen storage, wing-mounted fuel cell propulsion units, and the associated cooling and air supply lines.

The main technology assumptions adopted for the hydrogen fuel cell powerplant are summarized in Table 2. The tank system is assumed to be cryogenic, with vacuum and multi-layer insulation, hemispherical caps, Aluminium 2219 structural components, and insulation materials based on Dacron and double-aluminized polyester. For the liquid hydrogen tanks installed on all hydrogen-powered configurations investigated in this work, the design venting pressure is set equal to 2 bar, based on the outcome of the optimization studies reported in [13]. It should be noted that this value is adopted from a preliminary aircraft-level optimization of the storage system, mainly driven by tank mass, volume, and integration effects. At this stage, the tank pressure selection does not explicitly account for additional constraints associated with refuelling operations or with the pressure levels required by the hydrogen distribution system to supply the fuel cell system.

For the fuel cell system, gravimetric and volumetric power densities equal to 2.0 kW/kg and 2.0 kW/L are assumed, respectively. These values are used to estimate the mass and volume of the fuel cell system as a function of its design power. The fuel cell efficiency is assumed to vary with load, ranging from 55% at maximum power to 65% at the minimum considered operating power, set equal to 10% of the peak power. This load-dependent efficiency model is used to account, for a fuel cell system, for the improved efficiency generally expected at partial-load operation.

The air supply and cooling subsystems are sized through power density-based assumptions. The air supply line is assigned a gravimetric power density of 7.1 kW/kg, while the cooling line is assigned a gravimetric power density of 3.0 kW/kg. In the latter case, the sizing also accounts for the fuel cell efficiency, since the amount of heat to be rejected is directly related to the balance between the chemical power supplied by hydrogen and the useful electrical power delivered by the fuel cell system. In addition to their mass contribution, these auxiliary subsystems introduce power penalties

that depend on altitude. In the present study, the corresponding losses are represented through a linear trend, increasing from approximately 8% of the fuel cell system power at sea level to approximately 20% at 27,000 ft. For operating altitudes above 27,000 ft, the same trend is extrapolated.

The power line is modelled by assuming a gravimetric power density of 5.0 kW/kg for the electric motor, including the contributions of inverter and cabling. A constant overall power line efficiency of 94% is adopted to account for the losses between the fuel cell electrical output and the propeller shaft.

Table 2 – Main level-of-technology assumptions adopted for the full-electric hydrogen fuel cell powerplant.

Powerplant-related variable	Value
Hydrogen tank	
Hydrogen gravimetric energy density	33.3 kWh/kg
Tank technology	Cryogenic
Capability	240 min @ISA+40°C w/o venting
Insulation	Vacuum + multi-layer insulation
Number of tanks	2
Fuel cell system (FCS)	
Gravimetric power density	2.0 kW/kg
Volumetric power density	2.0 kW/L
Efficiency @max. power	55.0%
Efficiency @min. power	65.0%
Nominal voltage	850 V
FCS air supply line (ASL) and cooling line (CL)	
ASL gravimetric power density	7.1 kW/kg
CL gravimetric power density	3.0 kW/kg
FCS-generated heat % removed through the exhaust	10.0%
ASL+CL FCS power extraction @SL, ISA	8.0%
ASL+CL FCS power extraction @8500 m, ISA	19.0%
Power line (PL)	
Electric motor + inverter gravimetric + cables power density	5.0 kW/kg
Electric motor efficiency	96.0%
Inverter efficiency	99.0%
Cables efficiency	99.5%
Reduction gearbox efficiency	99.4%

Regarding airframe technology assumptions, the 2040 EIS hydrogen-powered aircraft concepts are assumed to benefit from the adoption of more advanced structural materials and manufacturing solutions compared to the 2020 EIS conventional reference aircraft. These assumptions are applied to the main structural components, including wing, horizontal and vertical tailplanes, fuselage, nacelles, landing gear structures, as well as to furnishing and equipment items. At component-level, the resulting mass reductions are assumed to be in the range of approximately 10–15% with respect to the corresponding components of a comparable 2020 EIS conventional aircraft.

Consistent with the same 2040 EIS scenario, aerodynamic improvements are also introduced for the hydrogen-powered variants. Refinements are applied to the zero-lift drag build-up, with specific attention to interference and excrescence drag contributions. Compared to the 2020 EIS conventional aircraft models, these two contributions are reduced by approximately 50% for the hydrogen-powered configurations. This assumption is intended to represent the expected benefits of improved aerodynamic design, cleaner external surfaces, reduced gaps and discontinuities, and more refined integration of aircraft component intersections.

An upper bound equal to 15 is imposed on the wing aspect ratio for all investigated configurations. This limit is introduced to avoid exploring wing designs for which aeroelastic effects may become a dominant sizing driver but are not explicitly captured with sufficient fidelity within the present conceptual design workflow. Very high-aspect-ratio cantilever wings may be significantly affected by static and dynamic aeroelastic phenomena, structural flexibility, and stiffness-driven mass penalties, which would require dedicated modelling beyond the current JPAD implementation. The selected upper limit therefore ensures that the optimization remains within a design space compatible with

the fidelity level of the adopted methods.

Concerning the SFC of gas turbine engines installed on conventional aircraft, a reference value of approximately 290 g/kWh, corresponding to an energy efficiency of about 28.5%, is assumed at sea-level static conditions for a rated shaft power of about 2,000 kW. This value is considered representative of state-of-the-art regional turboprop engines, such as those belonging to the Pratt & Whitney PW100 family and installed on aircraft comparable to the ATR 72-600. When the required engine shaft power deviates from the 2,000 kW reference value, the SFC is adjusted through a scaling law derived from publicly available data for different engine sizes within the PW100 turboprop family [18][19]. This correction accounts for size-related effects, leading to higher SFC values for smaller engines and lower SFC values for larger engines.

Regarding the number of installed propulsion units, all hydrogen-powered aircraft configurations are assumed to feature two engines per semi-wing, consistently with the outcomes of the optimization studies reported in [13]. For the conventional aircraft, instead, a preliminary assessment performed within the present work indicated that a configuration with one engine per semi-wing remains the most suitable solution.

2.3.2 Economic assumptions

The estimation of direct operating costs requires the definition of several input parameters, many of which are highly uncertain and subject to fluctuations driven by the economic, industrial, and political context. This uncertainty becomes even more relevant when future aircraft concepts and unconventional propulsion architectures are considered. In such cases, cost assumptions must be introduced for airframe and powerplant components that are still characterized by limited market readiness, scarce public data, or highly sensitive industrial information.

In the present work, the cost-related assumptions adopted for both conventional kerosene-powered and hydrogen fuel cell-powered aircraft are mainly derived from the European Clean Sky 2 project GENESIS[1] (*Gauging the ENvironmEntal Sustainability of electrIc aircraft Systems*). Within GENESIS, the University of Naples Federico II contributed to the development of a MATLAB-based tool for the estimation of direct operating costs of conventional, hybrid-electric, and full-electric aircraft, including battery- and fuel cell-based propulsion architectures, over three different time horizons: short-term, corresponding to 2025–2035; medium-term, corresponding to 2035–2045; and long-term, corresponding to 2045–2050+ [16][20]. In addition, a dedicated set of assumptions was defined for a state-of-the-art 2020 regional propeller-driven aircraft, representative of currently available turboprop aircraft and used as a reference benchmark.

Table 3 summarizes the main assumptions adopted for the DOC estimation of conventional turboprop and hydrogen fuel cell-powered aircraft. The former are based on the GENESIS assumptions for a 2020 state-of-the-art regional turboprop aircraft, while the latter are derived from the medium-term GENESIS assumptions for full-electric hydrogen-powered aircraft, with minor modifications and adaptations introduced where necessary to harmonize the comparison between the 2020 conventional and 2040 hydrogen-powered configurations investigated in this work. For input parameters that are particularly sensitive to economic and political scenarios, namely kerosene and hydrogen costs, the values reported in the table are not treated only as fixed reference assumptions. Instead, they are used as baseline values for subsequent parametric analyses, aimed at quantifying the sensitivity of operating costs to fuel price variations.

All monetary values are expressed in equivalent 2020 USD. When cost data or estimating relationships refer to different economic years, they are corrected through an inflation factor based on the ratio between the Consumer Price Index of 2020 and that of the original reference year, following the same general approach adopted by [16].

Table 3 – Main economic assumptions adopted for the 2020 conventional turboprop aircraft and the 2040 hydrogen-powered aircraft concepts investigated in this work.

	2020 state-of-the-art conventional aircraft	**2040 hydrogen-powered aircraft**	
Input variable	*Value*	*Value*	*Unit*
Typical mission range	250		nm

[1] https://www.genesis-cleansky.eu/

Kerosene price	1.06	-	2020 USD/kg
Hydrogen price	-	2.13	2020 USD/kg
Airframe spares	10% airframe price		%
Systems spares	10% systems price		%
Depreciation	20 years		-
Financing	85% of investment over 10 years		%
Insurance	1% of aircraft price per year		%
Turnaround time	0.50		h
Utilization	6		flights per day
Aircraft market price	Roskam's method		-
Thermal engine price	Roskam's method	-	-
Propeller price	Roskam's method		-
Fuel cell system price	-	356.4	2020 USD/kW
Electric motor price	-	60.0	2020 USD/kW
Power electronics price	-	260.0	2020 USD/kW
LH2 storage system	-	119.0	2020 USD/kg

3. Results and discussion

3.1 TLARs-1 set-related analyses

The analyses carried out for the TLARs-1 requirement set show that, for the 2040 EIS hydrogen-powered configuration, the selected design point is mainly driven by the take-off field length (TOFL) requirement and by the imposed upper limit on wing span. This behaviour is illustrated in Figure 3, where the feasible region is bounded by the intersection of these two active constraints. The optimum configuration, identified by minimizing the block hydrogen consumption over the 1,000-nm design mission, is located at this intersection. The resulting aircraft is characterized by a single fuel cell unit gross output power of 2,410 kW and a wing planform area of 101.57 m^2. Due to the 36 m wing span limitation, this corresponds to a maximum achievable wing aspect ratio of 12.76. The optimum aircraft has a design mission block hydrogen consumption of 1,405 kg, a maximum take-off mass (MTOM) of 46,384 kg, an operating empty mass (OEM) of 35,196 kg, and a final fuselage overall length of 37.03 m, after convergence of the hydrogen tank sizing and fuselage update loop. The corresponding wing loading, W/S, is 456.7 kg/m^2, while the power-to-weight ratio, P/W, is 175.7 W/kg, considering the actual shaft power available at the propeller, equal to 2,037 kW per propulsion unit.

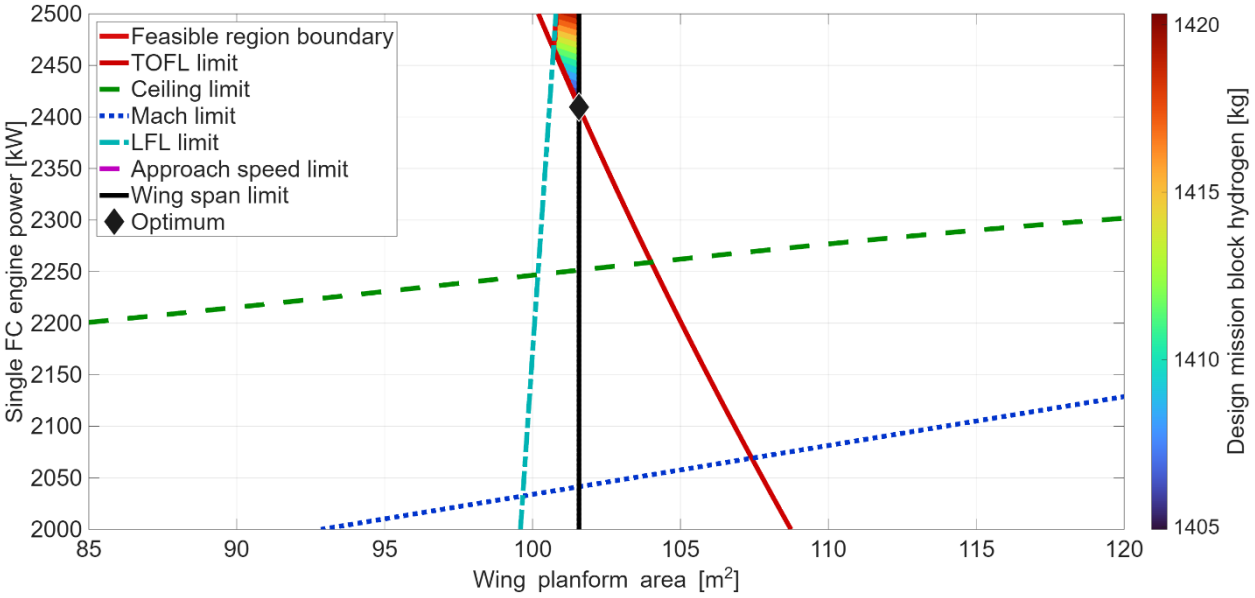


Figure 3 – Design mission block hydrogen contour and design-space constraints for the hydrogen-powered aircraft based on TLARs-1. The optimum configuration is found at a wing aspect ratio of 12.76, corresponding to the imposed 36 m wing span limit for ICAO Code C compatibility.

Figure 3 suggests that a relaxation of the ground performance requirements, particularly the TOFL constraint, can significantly enlarge the feasible design space and influence the optimal design selection. To assess this effect, the optimization was repeated by increasing both the TOFL and LFL requirements from 1,400 m to 1,500 m (TLARs-1.1). The resulting design space is shown in Figure 4, where the optimum configuration is shifted toward lower installed power and smaller wing area.

With the relaxed ground performance requirements, the optimum aircraft is characterized by a fuel cell system gross output power of 2,316 kW per propulsion unit, corresponding to an available shaft power at the propeller of 1,956 kW. The wing planform area is reduced to 95.34 m^2, which, under the imposed 36 m wing span limitation, corresponds to a maximum achievable wing aspect ratio of 13.59. Compared with the baseline TLARs-1 optimum, the reduction in both installed fuel cell power and wing area triggers a beneficial snowball effect on the aircraft sizing process, although part of this benefit is counteracted by the increase in wing mass resulting from the higher wing aspect ratio. The lower installed power and smaller wing overall reduce aircraft mass, which in turn decreases the thrust and energy demand during the mission. The reduced hydrogen requirement then leads to smaller tanks and a shorter fuselage, with further benefits in terms of mass and aerodynamic drag.

As a result, the optimum aircraft obtained with relaxed ground performance requirements has an MTOM of 45,550 kg, an OEM of 34,421 kg, and a final fuselage length of 36.77 m after convergence of the hydrogen storage integration loop. The final design is characterized by a W/S of 477.8 kg/m^2 and a P/W of 171.8 W/kg. The corresponding design mission block hydrogen consumption is 1,350 kg, representing a reduction of approximately 3.9% with respect to the baseline TLARs-1 optimum.

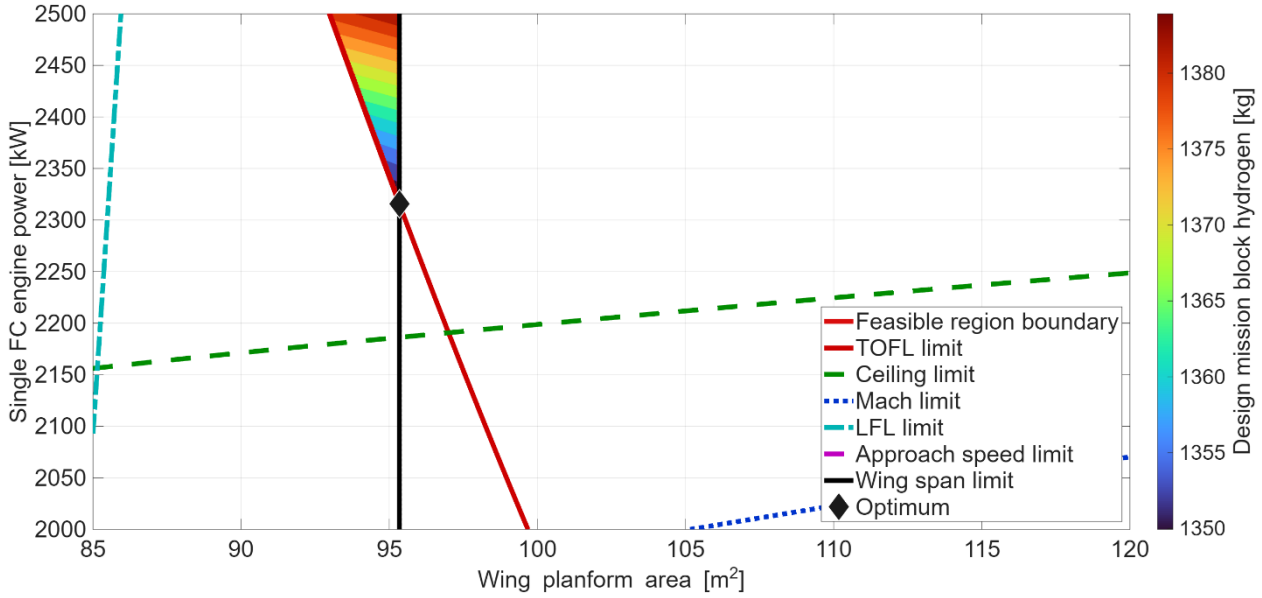


Figure 4 – Design mission block hydrogen contour and design space constraints for the TLARs-1.1 hydrogen-powered aircraft with relaxed ground performance requirements, corresponding to TOFL and LFL equal to 1,500 m. The optimum is located at the 36 m wing span limit, with a resulting wing aspect ratio of 13.59.

A further improvement can be obtained when the wing span constraint is relaxed together with the ground performance requirements (TLARs-1.2). This case is intended to represent the potential adoption of foldable wing tips, which would allow the aircraft to achieve a higher effective wing span and aspect ratio in flight while preserving compatibility with airport gate and taxiway limitations on ground. In principle, this solution would introduce an additional wing mass penalty associated with the folding mechanism, which can be estimated at conceptual design level [22]. However, in the present preliminary assessment, this additional mass penalty is not included; therefore, the results should be interpreted as an optimistic estimate of the potential benefit associated with wing span relaxation.

The results shown in Figure 5 indicate that, unlike the previous cases, the optimum is not located at the intersection of the active constraints. The minimum design mission block hydrogen consumption is obtained for a single fuel cell system gross output power of 2,213 kW, corresponding to an

available shaft power of 1,867 kW, and a wing planform area of 95.67 m^2. The optimum solution is found at a wing aspect ratio of 15, corresponding to the upper limit adopted in the present study, and results in a wing span of 37.88 m, i.e., 1.88 m above the 36 m ICAO Code C limit.

The corresponding aircraft has an MTOM of 44,897 kg and an OEM of 33,843 kg, with a final fuselage length of 36.50 m. The resulting W/S is 469.3 kg/m^2, while the P/W is 166.3 W/kg. The design mission block hydrogen consumption is reduced to 1,298 kg, corresponding to an additional reduction of approximately 3.9% with respect to the previous optimization case with relaxed ground performance requirements but fixed 36 m wing span limit.

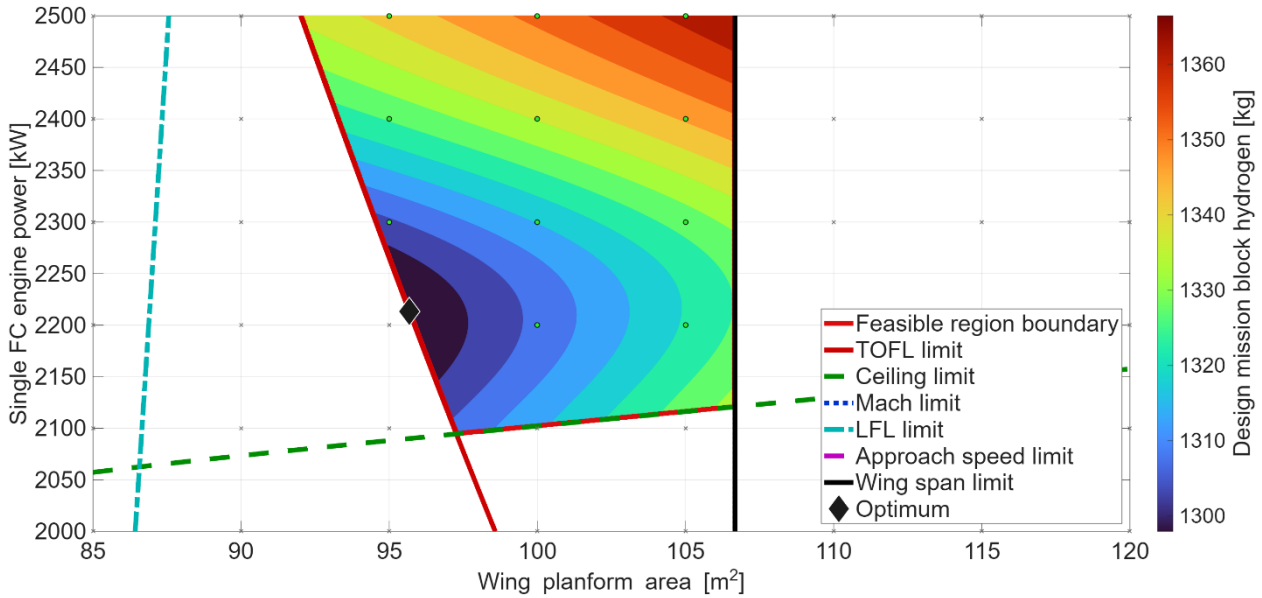


Figure 5 – Design mission block hydrogen contour and design space constraints for the TLARs-1.2 hydrogen-powered aircraft with relaxed ground performance requirements, corresponding to TOFL and LFL equal to 1,500 m, and relaxed wing span constraint enabled by foldable wing tips. The optimum is obtained at the upper aspect ratio limit adopted in this study, AR = 15.

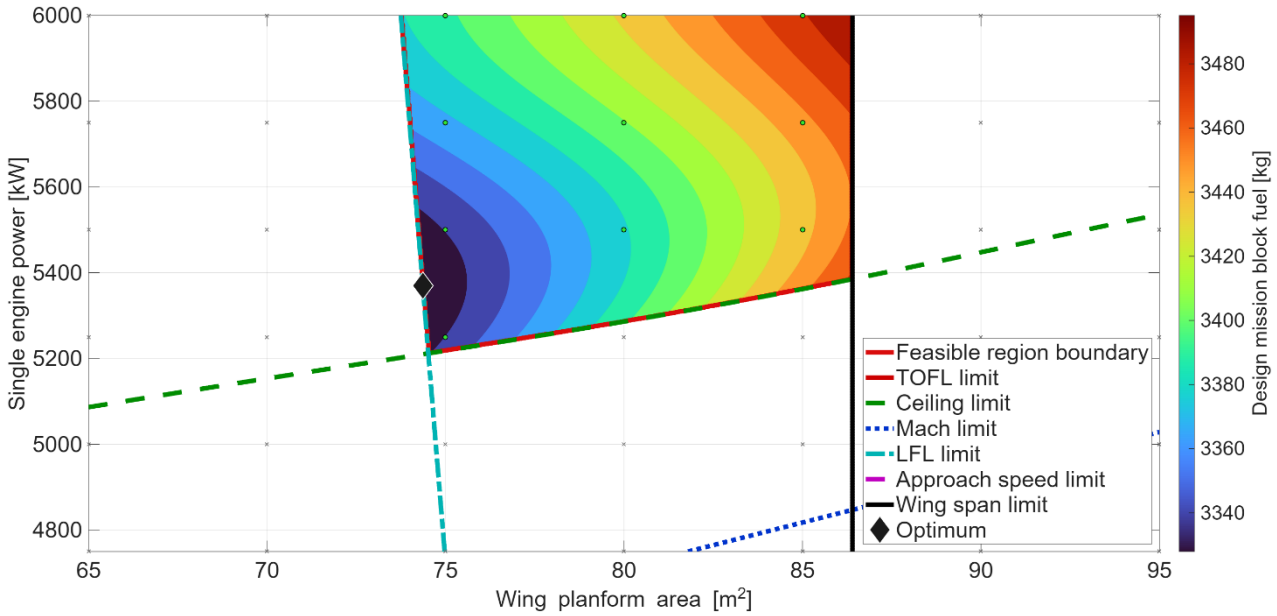
It is also useful to compare the previous hydrogen-powered configurations with the corresponding 2020 EIS conventional turboprop aircraft designed around the same TLARs-1 requirement set. This comparison highlights how the active design constraints and the response to requirement relaxation differ between hydrogen fuel cell propulsion and conventional gas turbine propulsion, and provides a consistent basis for comparing the two propulsion architectures, at TLAR parity, in terms of mission energy consumption and DOC.

Figure 6 illustrates the design spaces obtained for the conventional aircraft. Figure 6a refers to the baseline TLARs-1 requirements. In this case, the optimum configuration, identified by minimizing the kerosene consumption over the 1,000-nm design mission, is mainly constrained by the LFL requirement and is found at the upper aspect ratio limit adopted in this study, AR = 15. The resulting aircraft has a generated power per engine of 5,370 kW, corresponding to a maximum available shaft power of 5,276 kW. Considering the conventional aircraft arrangement with one engine per semi-wing, this leads to a total available shaft power of 10,552 kW. The optimum wing planform area is equal to 74.36 m^2, corresponding to a wing span of 33.40 m. The aircraft has an MTOM of 35,351 kg and an OEM of 21,628 kg, resulting in a W/S of 475.4 kg/m^2 and a P/W of 298.5 W/kg. The design mission block fuel consumption is equal to 3,328 kg.

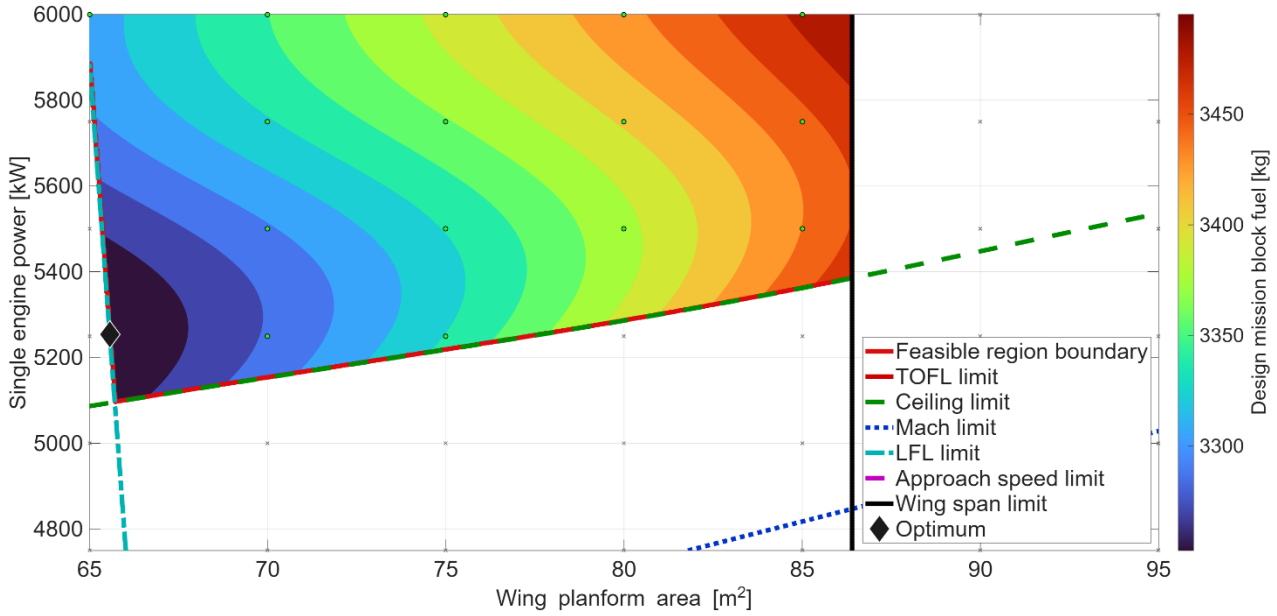
When the ground performance requirements are relaxed to 1,500 m for both TOFL and LFL (TLARs-1.1), as shown in Figure 6b, the optimum design shifts toward a smaller wing area and slightly lower installed power. The optimum wing planform area is reduced to 65.57 m^2, while the generated gas turbine power decreases to 5,253 kW, corresponding to an available shaft power of 5,160 kW per engine. The optimum wing AR remains equal to the upper cap of 15, leading to a wing span of 31.36 m. The resulting aircraft has an MTOM of 34,833 kg and an OEM of 21,197 kg, with a W/S of 531.2 kg/m^2 and a P/W of 296.3 W/kg. The design mission block fuel consumption decreases to 3,253 kg, corresponding to a reduction of approximately 2.3% with respect to the baseline TLARs-1

conventional optimum.

It is worth noting that, for the conventional aircraft, relaxing the maximum wing span constraint (TLARs-1.2) would not provide an additional benefit in the present design space. In both the baseline and relaxed ground performance cases, the optimum is already located at the imposed upper AR limit, while the corresponding wing spans remain below the 36 m ICAO Code C limit.



a)



b)

Figure 6 – Design mission block fuel contours and design space constraints for the TLARs-1 conventional turboprop aircraft: (a) baseline ground performance requirements (TLARs-1); (b) relaxed ground performance requirements, with TOFL and LFL equal to 1,500 m (TLAR-1.1). In both cases, the optimum is obtained at the upper aspect ratio limit adopted in this study, AR = 15, while remaining below the 36 m ICAO Code C wing span limit.

Table 4 summarizes the main characteristics and performance indicators of the conventional and hydrogen-powered aircraft designed around the TLARs-1 requirement set and its two relaxed variants. In all cases, the hydrogen-powered configurations require a significantly larger wing planform area than the corresponding conventional aircraft, with increases ranging from approximately 37% for the baseline TLARs-1 case to about 46% for the relaxed ground performance cases. This is mainly associated with the higher aircraft mass and the need to satisfy field

performance constraints while accommodating the additional mass and volume penalties introduced by the hydrogen fuel cell powertrain and storage system. The hydrogen-powered aircraft exhibit substantially higher MTOM and OEM values, with MTOM increases close to 29–31% and OEM increases close to 60–63% with respect to the conventional counterparts.

Despite these mass penalties, the hydrogen-powered configurations require lower total shaft power than the conventional turboprop aircraft. This result is mainly related to the different off-design behaviour of the two propulsion architectures. Conventional gas turbine engines are strongly affected by power lapse with altitude and flight condition, which may require a high sea-level installed power when cruise ceiling and maximum cruise Mach number requirements are demanding. In contrast, fuel cell electric propulsion is also affected by altitude-dependent losses, mainly associated with the air supply subsystem, but the corresponding power penalties are less severe than those typically experienced by gas turbine engines. As a result, the required installed shaft power at aircraft level is lower for the hydrogen-powered variants. For the TLARs examined in this case, Figure 6 also shows that the conventional engine sizing is not primarily driven by the take-off field length requirement, but rather by the combined effect of landing, cruise ceiling, and, to a lesser extent, cruise Mach number constraints.

From an energy perspective, the hydrogen-powered aircraft remain penalized with respect to the conventional aircraft when the comparison is performed on the basis of block energy per nautical mile and seat. For the baseline TLARs-1 case, the hydrogen-powered configuration shows a block energy increase of about 17.3%. However, this gap progressively decreases when the requirements are relaxed, reaching 15.3% for the relaxed ground performance case and 10.8% when the wing span constraint is also relaxed through the assumed use of foldable wing tips. This confirms that moderate relaxations in ground performance and wing span constraints can provide relevant benefits at aircraft level.

The DOC results show a strong dependence on the assumed fuel cost scenario. Under the baseline fuel cost assumptions (Table 3), the hydrogen-powered aircraft are only moderately penalized compared with the conventional configurations, with DOC increases between 2.8% and 3.6%. In the hydrogen-unfavourable scenario, characterized by low kerosene/high hydrogen cost (kerosene price of 0.51 2020 USD/kg and hydrogen price of 3.0 2020 USD/kg [16]), the DOC penalty increases substantially, reaching approximately 18–19%. Conversely, in the hydrogen-favourable scenario (kerosene price of 1.95 2020 USD/kg and hydrogen price of 1.35 2020 USD/kg [16]), the hydrogen-powered aircraft become economically advantageous, with DOC reductions of about 13–14% compared with the conventional aircraft. These results highlight that, for the TLARs-1 class of requirements, the economic competitiveness of hydrogen fuel cell aircraft is strongly linked not only to aircraft-level design improvements, but also to the future evolution of hydrogen and kerosene prices.

Table 4 – Comparison of the main sizing, performance, energy, and DOC indicators for the conventional turboprop and hydrogen-powered aircraft designed around TLARs-1 and its relaxed variants. Percentage differences are computed between the hydrogen-powered and conventional configurations for each requirement case.

	Requirements								
	TLARs-1			**TLARs-1.1[6]**			**TLARs-1.2[7]**		
	Conv.	**H2**	**Δ%[5]**	**Conv.**	**H2**	**Δ%[5]**	**Conv.**	**H2**	**Δ%[5]**
Wing area [m^2]	74.36	101.57	+36.6	65.57	95.34	+45.4	65.57	95.67	+45.9
Wing AR [-]	15.0	12.76	-	15.0	13.59	-	15.0	15.0	-
Wing span [m]	33.4	36.0	-	31.36	36.0	-	31.36	37.88	-
Total shaft power [kW]	10,552	8,148	-22.8	10,320	7,824	-24.2	10,320	7,468	-27.6
MTOM [kg]	35,351	46,384	+31.2	34,833	45,550	+30.8	34,833	44,897	+28.9
OEM [kg]	21,628	35,196	+62.7	21,197	34,421	+62.4	21,197	33,843	+59.7

W/S [kg/m^2]	475.4	456.7	-3.9	531.2	477.8	-10.1	531.2	469.3	-11.7
P/W [W/kg]	298.5	175.7	-41.1	296.3	171.8	-42.0	296.3	166.3	-43.9
Block energy[1] [Wh/ (nm seat)]	399.36	468.29	+17.3	390.36	450.0	+15.3	390.36	432.62	+10.8
Total DOC (sc. 1)[2] [¢$/ (nm seat)]	21.69	22.48	+3.6	21.38	22.16	+3.6	21.38	21.97	+2.8
Total DOC (sc. 2)[3] [¢$/ (nm seat)]	19.86	23.71	+19.4	19.60	23.34	+19.1	19.60	23.11	+17.9
Total DOC (sc. 3)[4] [¢$/ (nm seat)]	24.65	21.39	-13.2	24.28	21.12	-13.0	24.28	20.97	-13.6

[1] Values are referred to the 1,000-nm design mission and are computed assuming lower heating values of 12 kWh/kg for kerosene and 33.33 kWh/kg for hydrogen.
[2] Baseline fuel-cost scenario, based on the kerosene and hydrogen prices reported in Table 3.
[3] Hydrogen-unfavourable cost scenario envisaged for 2040 in [16], assuming a kerosene price of 0.51 2020 USD/kg and a hydrogen price of 3.00 2020 USD/kg.
[4] Hydrogen-favourable cost scenario envisaged for 2040 in [16], assuming a kerosene price of 1.95 2020 USD/kg and a hydrogen price of 1.35 2020 USD/kg.
[5] Percentage variations are computed as relative differences between the hydrogen-powered and conventional configurations for each requirement case.
[6] Relaxed ground-performance requirements with respect to TLARs-1, with TOFL and LFL increased from 1,400 m to 1,500 m.
[7] Relaxed wing span constraint with respect to TLARs-1.1, representing the assumed adoption of foldable wing tips.

3.2 TLARs-2 set-related analyses

Table 5 summarizes the main sizing, performance, energy, and DOC indicators obtained for the TLARs-2 requirement set and its variants. Compared with TLARs-1, this second requirement set represents a less demanding operational scenario in terms of payload, cruise altitude, and cruise Mach number, while retaining the same 1,000-nm design range. As a result, both conventional and hydrogen-powered configurations are generally characterized by lower aircraft masses and lower installed power levels than those obtained for TLARs-1.

For the baseline TLARs-2 case, the optimum hydrogen-powered configuration is still constrained by the 36 m wing span limitation. The design-space analysis shows that the optimum is located at the intersection between the TOFL constraint and the wing span limit, leading to a wing aspect ratio of 13.38 (Figure 7). When the ground performance requirements are made stricter by reducing both TOFL and LFL from 1,400 m to 1,300 m (TLARs-2.1), the feasible region becomes significantly more restricted. In this case, the optimum hydrogen-powered solution is essentially reduced to the intersection of TOFL, LFL, and wing span constraints, resulting in a lower aspect ratio of 12.42 and a higher wing area. When the wing span constraint is subsequently relaxed (TLARs-2.2), representing the assumed use of foldable wing tips, the hydrogen-powered optimum moves toward the upper AR limit adopted in this study, with a wing span of 40.79 m. In this case, the optimum is mainly governed by the interaction between the TOFL and cruise ceiling constraints (Figure 8).

The conventional aircraft show a different constraint behaviour. For the baseline TLARs-2 case, the optimum is primarily driven by the approach speed requirement, while the aspect ratio reaches the imposed upper cap of 15 without exceeding the 36 m wing span limit. When the ground performance requirements are tightened, the landing field length constraint becomes more relevant, together with the cruise ceiling limitation. As already observed for TLARs-1, relaxing the wing span constraint does not provide an additional benefit for the conventional aircraft, since the optimum is already located at the maximum allowed aspect ratio while remaining below the ICAO Code C wing span limit.

From a sizing perspective, the hydrogen-powered aircraft remain heavier than the corresponding conventional aircraft, although the relative penalties are lower than those observed for TLARs-1. The MTOM increase ranges from approximately 19% to 24%, while the OEM increase ranges from about 44% to 52%. The largest reduction in the mass penalty is obtained when the wing span constraint is relaxed, since the higher aspect ratio allows a more efficient aircraft configuration and reduces both mission hydrogen demand and storage-related sizing penalties.

The energy comparison shows a clear improvement with respect to TLARs-1. For the baseline TLARs-2 case, the hydrogen-powered aircraft requires only about 3.4% more block energy per nautical mile and seat than the conventional aircraft. When the ground performance requirements

are made stricter, the energy penalty increases to about 5.8%, mainly because the hydrogen-powered design is forced toward a less favourable constrained solution. Conversely, when the wing span constraint is relaxed, the hydrogen-powered aircraft becomes slightly more energy-efficient than the conventional counterpart, with a block energy reduction of about 2.1%.

The DOC results also indicate a more favourable trend for hydrogen-powered aircraft than in the TLARs-1 case. Under the baseline fuel cost scenario, the hydrogen-powered configurations show slightly lower DOC values than the conventional aircraft for all TLARs-2 variants, with reductions between approximately 0.6% and 2.6%. In the hydrogen-unfavourable fuel cost scenario, the conventional aircraft remain economically preferable, with hydrogen DOC penalties of about 11–14%. Conversely, in the hydrogen-favourable scenario, the hydrogen-powered aircraft show a significant DOC advantage, with reductions of approximately 16–18%.

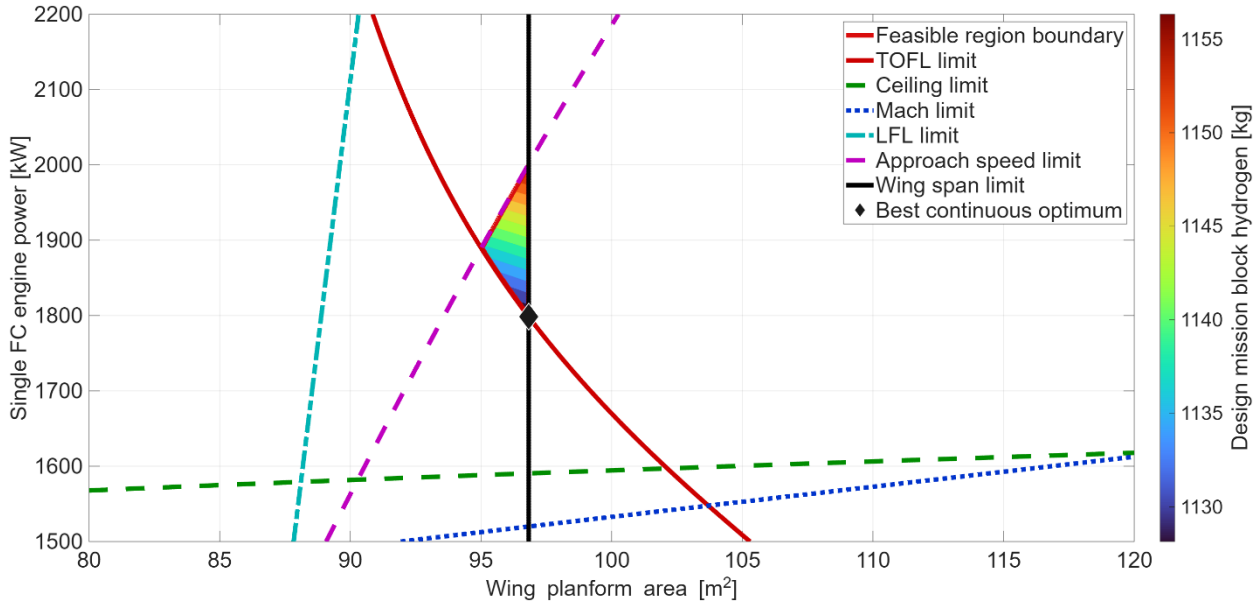


Figure 7 – Design mission block hydrogen contour and design space constraints for the hydrogen-powered aircraft based on TLARs-2. The optimum configuration is found at a wing aspect ratio of 13.38, corresponding to the imposed 36 m wing span limit for ICAO Code C.

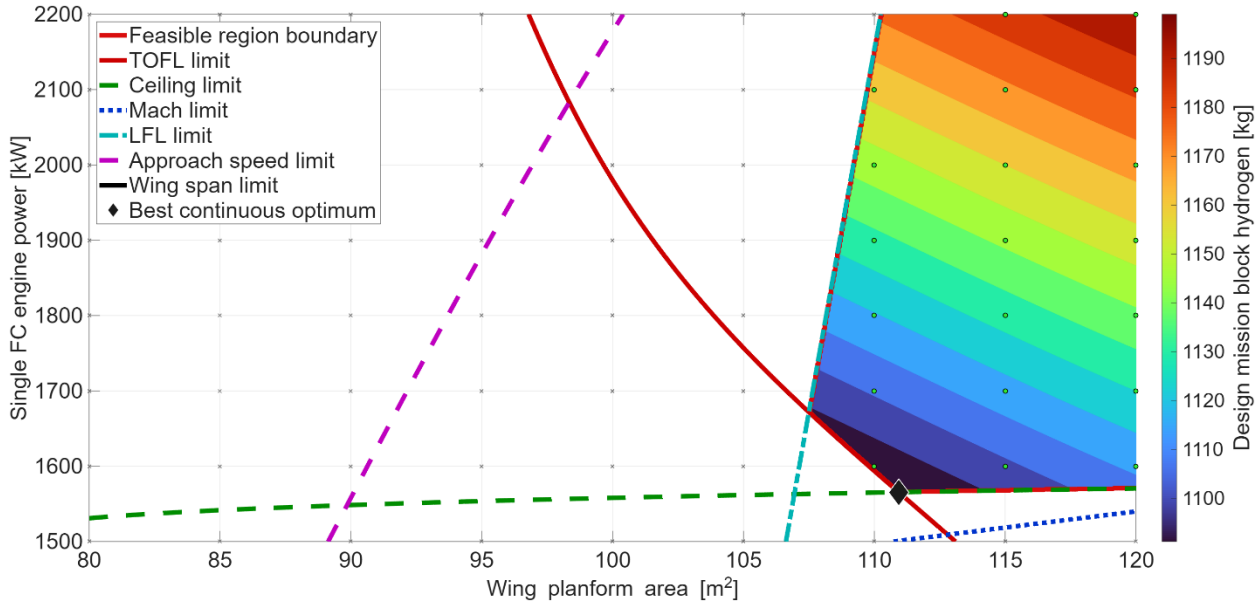


Figure 8 – Design mission block hydrogen contour and design space constraints for the TLARs-2.2 hydrogen-powered aircraft with stricter ground performance requirements, corresponding to TOFL and LFL equal to 1,300 m, and relaxed wing span constraint enabled by foldable wing tips. The optimum is obtained at the upper aspect ratio limit adopted in this study, AR = 15.

Table 5 – Comparison of the main sizing, performance, energy, and DOC indicators for the conventional turboprop and hydrogen-powered aircraft designed around TLARs-2 and its variants. Percentage differences are computed between the hydrogen-powered and conventional configurations for each requirement case.

	Requirements								
	TLARs-2			TLARs-2.1[6]			TLARs-2.2[7]		
	Conv.	H2	Δ%[5]	Conv.	H2	Δ%[5]	Conv.	H2	Δ%[5]
Wing area [m^2]	73.52	96.83	+31.7	80.16	104.33	+30.2	80.16	110.93	+38.4
Wing AR [-]	15.0	13.38	-	15.0	12.42	-	15.0	15.0	-
Wing span [m]	33.21	36.0	-	34.68	36.0	-	34.68	40.79	-
Total shaft power [kW]	8,090	6.032	-25.4	8,300	6,288	-24.2	8,300	5,224	-37.1
MTOM [kg]	31,884	39,422	+23.6	32,277	40,156	+24.4	32,277	38,398	+19.0
OEM [kg]	19,499	29,520	+51.4	19,826	30,197	+52.3	19,826	28,572	+44.1
W/S [kg/m^2]	433.68	407.13	-6.1	402.66	384.89	-4.4	402.66	346.15	-14.0
P/W [W/kg]	253.73	153.01	-39.7	257.15	156.59	-39.1	257.15	136.05	-47.1
Block energy[1] [Wh/ (nm seat)]	404.09	417.76	+3.4	412.77	436.68	+5.8	412.77	404.05	-2.1
Total DOC (sc. 1)[2] [¢$/ (nm seat)]	22.48	22.01	-2.1	22.76	22.62	-0.6	22.76	22.16	-2.6
Total DOC (sc. 2)[3] [¢$/ (nm seat)]	20.63	23.11	+12.0	20.87	23.77	+13.9	20.87	23.22	+11.3
Total DOC (sc. 3)[4] [¢$/ (nm seat)]	25.48	21.04	-17.4	25.82	21.61	-16.3	25.82	21.22	-17.8

[1] Values are referred to the 1,000-nm design mission and are computed assuming lower heating values of 12 kWh/kg for kerosene and 33.33 kWh/kg for hydrogen.
[2] Baseline fuel-cost scenario, based on the kerosene and hydrogen prices reported in Table 3.
[3] Hydrogen-unfavourable cost scenario envisaged for 2040 in [16], assuming a kerosene price of 0.51 2020 USD/kg and a hydrogen price of 3.00 2020 USD/kg.
[4] Hydrogen-favourable cost scenario envisaged for 2040 in [16], assuming a kerosene price of 1.95 2020 USD/kg and a hydrogen price of 1.35 2020 USD/kg.
[5] Percentage variations are computed as relative differences between the hydrogen-powered and conventional configurations for each requirement case.
[6] Stricter ground-performance requirements with respect to TLARs-2, with TOFL and LFL reduced from 1,400 m to 1,300 m.
[7] Relaxed wing span constraint with respect to TLARs-2.1, representing the assumed adoption of foldable wing tips.

3.3 TLARs-3 set-related analyses

Table 6 summarizes the main results obtained for the TLARs-3 requirement set and its variants. This third requirement set represents the least demanding operational scenario considered in the present study, with reduced design payload, shorter design range, lower cruise altitude, and lower cruise Mach number compared with TLARs-1 and TLARs-2. As a result, both conventional and hydrogen-powered configurations are characterized by lower aircraft masses and installed power levels, making TLARs-3 particularly useful for assessing whether hydrogen fuel cell propulsion becomes more competitive when the aircraft requirements are closer to current regional turboprop operations.

For the baseline TLARs-3 case, the design space analysis shows that the optimum hydrogen-powered configuration is found at the intersection of the LFL, TOFL, and wing span constraints. The corresponding wing aspect ratio remains below the upper cap adopted in this work, with AR = 14.14 and a wing span equal to the 36 m ICAO Code C limit. When the ground performance requirements are made stricter by reducing both TOFL and LFL from 1,300 m to 1,200 m (TLARs-3.1), the optimum remains strongly constrained by field performance and wing span, and the hydrogen-powered aircraft is forced toward a larger wing area and lower aspect ratio. In the variant with relaxed wing

span constraint (TLARs-3.2), representing the assumed use of foldable wing tips, the optimum moves to the upper aspect ratio limit of the investigated design space, with a wing span of 41.12 m. In this case, the optimum feasible solution is mainly located by the interaction between the TOFL and maximum cruise Mach number constraints, while the LFL requirement still contributes to restricting the available design space (Figure 9).

The conventional aircraft exhibit a different constraint behaviour. For the baseline TLARs-3 case, the optimum feasible solution is found at the intersection between the LFL and maximum cruise Mach number constraints. When the ground performance requirements are made stricter, the same qualitative behaviour is maintained, although the design point shifts toward larger wing area and higher engine power. As observed for the previous requirement sets, relaxing the wing span constraint is not relevant for the conventional aircraft, since the optimum already remains within the 36 m ICAO Code C limit even without foldable wing tips.

From a sizing perspective, the hydrogen-powered aircraft remain heavier than the corresponding conventional configurations, but the relative penalties are generally lower than those observed for the more demanding TLARs-1 and TLARs-2 cases. The MTOM increase ranges from approximately 17% to 24%, while the OEM increase ranges from about 39% to 51%. The lowest mass penalties are obtained when the wing span constraint is relaxed, since the higher aspect ratio enables a more efficient aerodynamic solution and reduces the hydrogen storage and propulsion system sizing burden.

The energy results indicate a clear improvement in favour of hydrogen-powered aircraft for this requirement set. Unlike TLARs-1 and TLARs-2, the hydrogen-powered configurations show lower block energy per nautical mile and seat than the conventional counterparts in all three TLARs-3 variants. The reduction is about 5.6% for the baseline TLARs-3 case and remains close to 4.9% when stricter ground performance requirements are imposed. When the wing span constraint is relaxed, the energy advantage increases to approximately 10.5%. This confirms that lower cruise speed, lower cruise altitude, reduced payload, and shorter range are more favourable to hydrogen fuel cell propulsion, especially when geometric constraints do not excessively limit the achievable wing aspect ratio.

The DOC results, however, show that this energy advantage does not automatically translate into an economic advantage under all fuel cost assumptions. In the baseline fuel cost scenario, the hydrogen-powered aircraft still exhibit higher DOC values than the conventional aircraft, with penalties decreasing from about 7.1% for the baseline TLARs-3 case to approximately 3.3% when the wing span constraint is relaxed. In the hydrogen-unfavourable scenario, the DOC penalty remains significant, ranging from about 19% to 24%. Conversely, in the hydrogen-favourable scenario, the hydrogen-powered aircraft become economically advantageous, with DOC reductions between approximately 10.6% and 14.0%. Therefore, TLARs-3 confirms that less demanding regional-aircraft requirements can make hydrogen fuel cell aircraft competitive from an energy standpoint, while their economic competitiveness remains strongly dependent on the future relative cost of hydrogen and kerosene.

Table 6 – Comparison of the main sizing, performance, energy, and DOC indicators for the conventional turboprop and hydrogen-powered aircraft designed around TLARs-3 and its variants. Percentage differences are computed between the hydrogen-powered and conventional configurations for each requirement case.

	Requirements								
	TLARs-3			**TLARs-3.1[6]**			**TLARs-3.2[7]**		
	Conv.	**H2**	**Δ%[5]**	**Conv.**	**H2**	**Δ%[5]**	**Conv.**	**H2**	**Δ%[5]**
Wing area [m^2]	69.57	91.66	+31.8	85.69	107.15	+25.0	85.69	112.75	+31.6
Wing AR [-]	15.0	14.14	-	15.0	12.09	-	15.0	15.0	-
Wing span [m]	32.30	36.0	-	35.85	36.0	-	35.85	41.12	-
Total shaft power [kW]	5,362	5,244	-2.2	5,745	4,800	-16.4	5,745	4,252	-26.0

MTOM [kg]	27,805	34,588	+24.4	28,672	34,243	+19.4	28,672	33,577	+17.1
OEM [kg]	17,250	26,020	+50.8	17,967	25,635	+42.7	17,967	25,043	+39.4
W/S [kg/m^2]	399.67	377.35	-5.6	334.60	319.58	-4.5	334.60	297.80	-11.0
P/W [W/kg]	192.84	151.61	-21.4	200.37	140.17	-30.0	200.37	126.63	-36.8
Block energy[1] [Wh/ (nm seat)]	436.23	411.85	-5.6	462.74	439.98	-4.9	462.74	414.04	-10.5
Total DOC (sc. 1)[2] [¢$/ (nm seat)]	21.68	23.23	+7.1	22.49	23.39	+4.0	22.49	23.24	+3.3
Total DOC (sc. 2)[3] [¢$/ (nm seat)]	19.68	24.32	+23.6	20.37	24.55	+20.5	20.37	24.33	+19.4
Total DOC (sc. 3)[4] [¢$/ (nm seat)]	24.92	22.28	-10.6	25.92	22.37	-13.7	25.92	22.28	-14.0

[1] Values are referred to the 800-nm design mission and are computed assuming lower heating values of 12 kWh/kg for kerosene and 33.33 kWh/kg for hydrogen.
[2] Baseline fuel-cost scenario, based on the kerosene and hydrogen prices reported in Table 3.
[3] Hydrogen-unfavourable cost scenario envisaged for 2040 in [16], assuming a kerosene price of 0.51 2020 USD/kg and a hydrogen price of 3.00 2020 USD/kg.
[4] Hydrogen-favourable cost scenario envisaged for 2040 in [16], assuming a kerosene price of 1.95 2020 USD/kg and a hydrogen price of 1.35 2020 USD/kg.
[5] Percentage variations are computed as relative differences between the hydrogen-powered and conventional configurations for each requirement case.
[6] Stricter ground-performance requirements with respect to TLARs-3, with TOFL and LFL reduced from 1,300 m to 1,200 m.
[7] Relaxed wing span constraint with respect to TLARs-3.1, representing the assumed adoption of foldable wing tips.

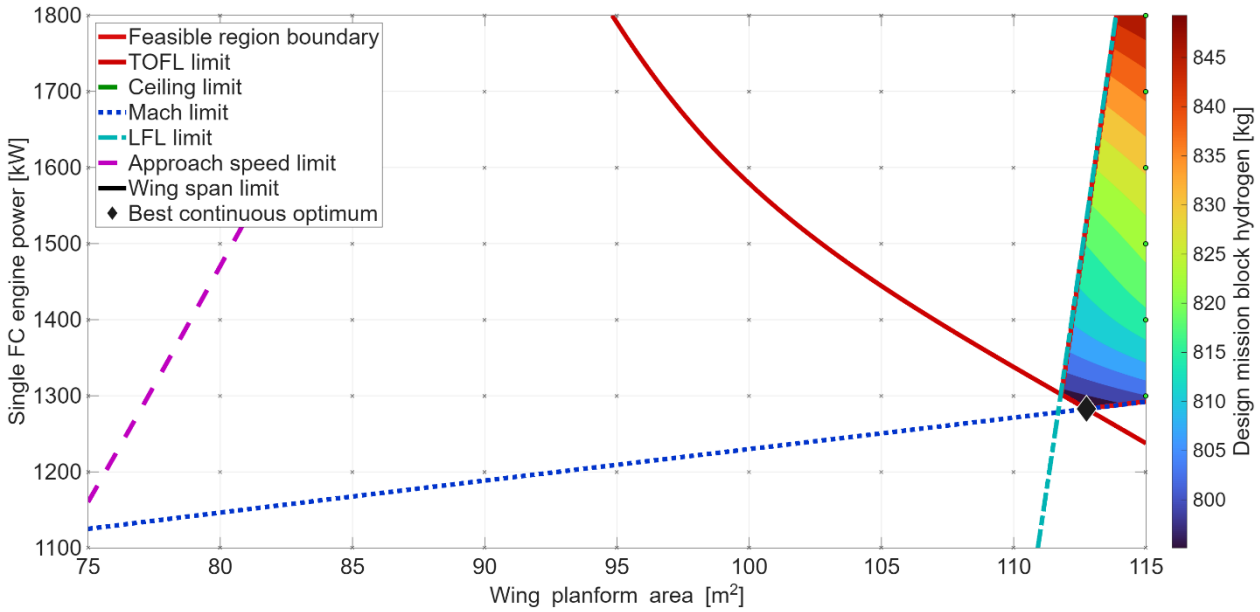


Figure 9 – Design mission block hydrogen contour and design space constraints for the TLARs-3.2 hydrogen-powered aircraft with stricter ground performance requirements, corresponding to TOFL and LFL equal to 1,200 m, and relaxed wing span constraint enabled by foldable wing tips. The optimum is obtained at the upper aspect ratio limit adopted in this study, AR = 15.

3.4 Comparison of requirement sets

The results presented in the previous subsections show that the relative attractiveness of hydrogen fuel cell propulsion is strongly dependent on the adopted TLARs. Figure 10 summarizes this behaviour by comparing all optimized conventional and hydrogen-powered configurations in terms of design mission block energy per nautical mile and seat, and total DOC per nautical mile and seat, for the three fuel cost scenarios considered in this work. The same data are reported in Table 4, Table 5, and Table 6, which provide the corresponding sizing and performance indicators for each requirement set and variant.

The TLARs-1 set represents the most demanding operational scenario investigated in this study and is closely aligned with the reference requirements adopted within the FAME project. TLARs-1 should be interpreted as an ambitious reference target for a hydrogen-powered regional aircraft intended to preserve a high level of operational capability. In particular, TLARs-1 combines the highest payload, design range, cruise altitude, and cruise Mach number among the investigated cases. These requirements provide clear operational advantages, as they allow the aircraft to address a broader and more demanding mission envelope. However, this ambition comes at aircraft-design level with penalties for the hydrogen-powered configuration. Compared with the corresponding conventional aircraft, the TLARs-1 hydrogen-powered designs show the largest MTOM and OEM increases, as well as the highest block energy per nautical mile and seat. Even when ground performance requirements are relaxed and the wing span constraint is unlocked, the hydrogen-powered TLARs-1.2 configuration remains penalized by about 10.8% in block energy with respect to its conventional counterpart. Therefore, TLARs-1 can be considered a valuable high-capability reference case, but also the most challenging one for hydrogen fuel cell propulsion under the technology assumptions adopted in this work.

The TLARs-3 set, at the opposite end of the investigated range, is closer to current regional turboprop operations, with lower payload, shorter design range, lower cruise altitude, and lower cruise Mach number. These characteristics are particularly favourable from an energy standpoint. Indeed, the hydrogen-powered TLARs-3 configurations show lower block energy per nautical mile and seat than the corresponding conventional aircraft for all investigated variants. The advantage ranges from about 4.9–5.6% for the baseline and more stringent ground performance cases, to approximately 10.5% when the wing span constraint is relaxed. This confirms that hydrogen fuel cell aircraft benefit from less demanding cruise requirements and shorter design ranges, which reduce installed power, mission energy demand, and hydrogen storage penalties. However, the DOC results show a more nuanced picture. Despite the favourable energy behaviour, the hydrogen-powered TLARs-3 configurations remain more expensive than their conventional counterparts in the baseline fuel cost scenario, with DOC penalties between about 3.3% and 7.1%. This indicates that, for smaller and less demanding aircraft, the conventional benchmark also becomes highly efficient and cost effective, while the capital and energy-carrier cost contributions associated with the hydrogen fuel cell powertrain remain significant.

The TLARs-2 set provides an intermediate scenario and appears to offer the best overall compromise among the investigated requirement families. Compared with TLARs-1, it relaxes payload, cruise altitude, and cruise Mach number while retaining the same 1,000-nm design range. As a result, the hydrogen-powered TLARs-2 configurations exhibit substantially reduced penalties relative to the conventional counterparts. In the baseline TLARs-2 case, the block energy penalty is limited to about 3.4%, while the baseline DOC is already slightly lower than for the corresponding conventional aircraft. When the wing span constraint is relaxed, the hydrogen-powered TLARs-2.2 configuration becomes slightly more efficient than the conventional counterpart in terms of block energy, with a reduction of about 2.1%, while also retaining a DOC advantage in the baseline cost scenario. At the same time, TLARs-2 preserves a more capable operational envelope than TLARs-3, especially in terms of design range, payload, cruise altitude, and cruise speed.

The effect of ground performance requirements also deserves specific attention. Shorter take-off and landing field lengths are operationally attractive because they increase the number of airports from which the aircraft can operate and improve network flexibility. This is especially relevant for regional aviation, where access to smaller airports can be an important requirement. However, the results show that this objective must be balanced against aircraft-level performance and efficiency. Tightening TOFL and LFL generally forces the optimum design toward larger wing areas and/or higher installed power, with associated mass and energy penalties. This effect is particularly visible for the hydrogen-powered configurations, where additional mass can trigger a snowball effect involving the fuel cell system, hydrogen storage, and aircraft sizing. Therefore, field-performance requirements should not be defined independently from the overall aircraft design objective; instead, they should be selected by considering the trade-off between airport accessibility, aircraft mass, mission energy, and DOC.

The wing span constraint represents another important driver for hydrogen-powered configurations. In several cases, especially for TLARs-1 and TLARs-2, the optimum hydrogen-powered aircraft is constrained by the 36 m ICAO Code C wing span limit. Relaxing this constraint through the assumed use of foldable wing tips allows higher aspect-ratio wings to be exploited and leads to reductions in

installed power, aircraft mass, and mission energy. The benefit is particularly relevant for TLARs-2, where the relaxed-span variant provides the best energy performance within its respective requirement family. Nevertheless, these results should be interpreted as optimistic, since the additional structural mass and system complexity associated with the folding mechanism have not been included in the present analysis.

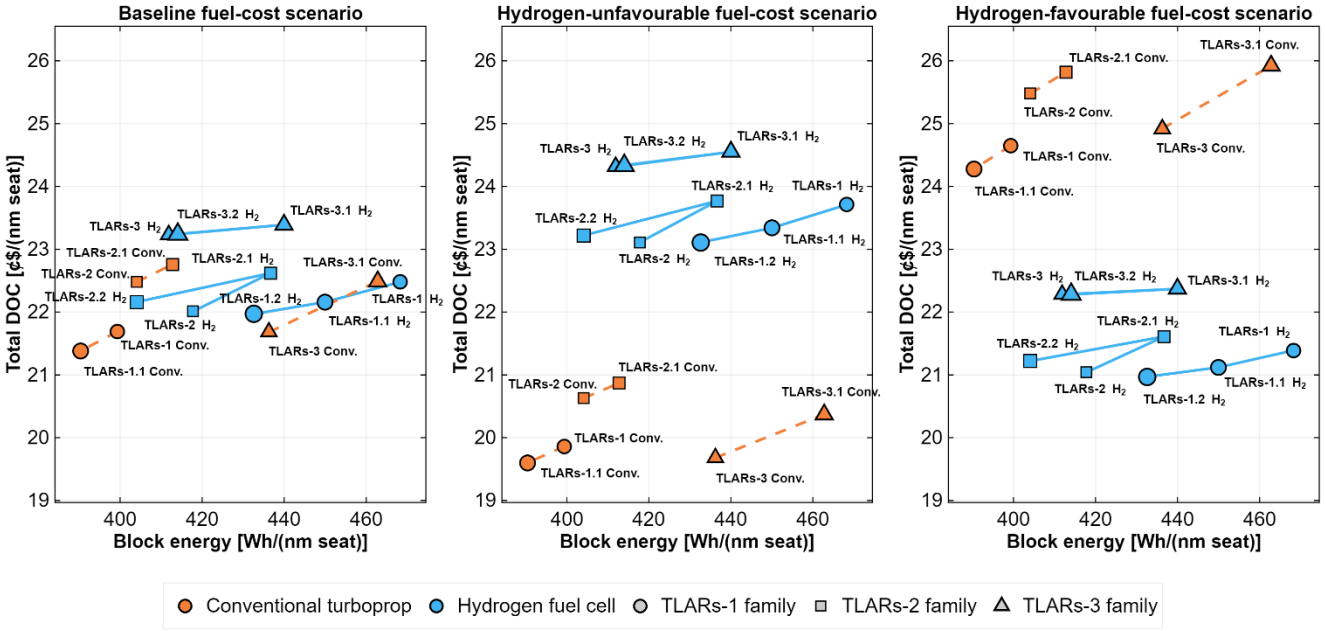


Figure 10 – Cross-comparison of optimized conventional kerosene-based turboprop and hydrogen-powered configurations in terms of design mission block energy and total DOC per nautical mile and seat for the three fuel cost scenarios considered in this work. Marker colour identifies the propulsion architecture, while marker shape and size identify the TLAR family and variant.

4. Conclusions

This paper investigated the influence of top-level aircraft requirements on the conceptual design of hydrogen fuel cell-powered regional aircraft. Three representative TLAR sets were considered, ranging from a FAME-oriented reference scenario to a set of requirements closer to current regional turboprop operations. For each requirement set and selected variants, optimized hydrogen-powered aircraft were compared with conventional turboprop counterparts designed around the same operational requirements but representative of current 2020 technology. The comparison was performed in terms of aircraft sizing, installed power, mass breakdown, block energy, and direct operating costs.

Overall, the comparison indicates that no single requirement set is universally preferable. TLARs-1 is the most ambitious and operationally capable case, but it is also the most demanding for hydrogen fuel cell propulsion. TLARs-3 is the most favourable from a pure energy consumption perspective, but its economic advantage is less evident under baseline fuel cost assumptions, and its operational capability is more limited. TLARs-2 offers the most favourable compromise between operational ambition, aircraft-level feasibility, energy consumption, and DOC. Under the level-of-technology assumptions adopted in this work, it appears to provide the most balanced starting point for a hydrogen fuel cell regional aircraft, especially when moderate relaxation of geometric constraints can be considered.

Future work should address additional aspects that were only partially captured in the present conceptual design study. These include a more detailed assessment of foldable wing-tip mass penalties, refinement of hydrogen storage and distribution assumptions, including refuelling feasibility and fuel cell supply-pressure constraints, and broader sensitivity analyses on fuel prices and technology KPIs.

5. Contact Author Email Address

mailto: mario.distasio@unina.it

6. Copyright Statement

The authors confirm that they, and/or their company or organization, hold copyright on all of the original material included in this paper. The authors also confirm that they have obtained permission, from the copyright holder of any third party material included in this paper, to publish it as part of their paper. The authors confirm that they give permission, or have obtained permission from the copyright holder of this paper, for the publication and distribution of this paper as part of the ICAS proceedings or as individual off-prints from the proceedings.

7. Acknowledgments

The research presented in this paper has been performed in the framework of the FAME (Fuel cell propulsion system for Aircraft Megawatt Engines) and has received funding from the European Union Clean Aviation program under Grant Agreement n° 101140559. The authors gratefully acknowledge the contributions and feedback received from all members of the FAME consortium throughout the course of this study.



8. References

[1] Nicolay S, Karpuk S, Liu Y, and Elham A. Conceptual design and optimization of a general aviation aircraft with fuel cells and hydrogen. *International Journal of Hydrogen Energy*, Vol 46, 2021.

[2] Svensson C, Oliveira A, and Gronstedt T. Hydrogen fuel cell aircraft for the Nordic market. *International Journal of Hydrogen Energy*, Vol. 61, 2024.

[3] Massaro M, Pramotton S, Marocco P, Monteverde A, and Santarelli M. Optimal design of a hydrogen-powered fuel cell system for aircraft applications. *Energy Conversion and Management*, Vol 306, 2024.

[4] Schroder M, Becker F, and Gentner C. Optimal design of proton exchange membrane fuel cell systems for regional aircraft. *Energy Conversion and Management*, Vol. 308, 2024.

[5] Quaium F, Bielsky T, and Thielecke F. Fuel cell cooling system design for hydrogen-powered concept aircraft. *Proc Deutscher Luft- und Raumfahrtkongress (DLRK) 2022*, Dresden, Germany, 27-29 September, 2022.

[6] Ahluwalia R, Wang X, Shah A, Lauer M, and Ansell P. Fuel cells for single-aisle regional aircraft: System configuration, performance and cost. *International Journal of Hydrogen Energy*, Vol. 159, 2025.

[7] Trifari V, Ruocco M, Cusati V, Nicolosi F, and De Marco A. Multi-disciplinary analysis and optimization Java tool for aircraft design. *Proc 31st Congress of the International Council of the Aeronautical Sciences (ICAS 2018)*, Belo Horizonte, Brazil, 9-14 September, 2018.

[8] De Marco A, Di Stasio M, Della Vecchia P, Trifari V, and Nicolosi F. Automatic modeling of aircraft external geometries for preliminary design workflows. *Aerospace Science and Technology*, Vol. 8, 2020.

[9] De Marco A, Trifari V, Nicolosi F and Ruocco M. A simulation-based performance analysis tool for aircraft design workflows. *Aerospace*, Vol. 7, No. 11, 2020.

[10] Prajwal P, Ciampa PD, Della Vecchia P, Ciliberti D, Voskuij M, Charbonnier D, Jungo A, Zhang M, Fioriti M, Anisimov K, and Mirzoyan A. Model based collaborative design & optimization of blended wing body aircraft configuration: AGILE EU project. *Proc 2018 Aviation Technology, Integration, and Operations Conference*, Atlanta, Georgia, 25-29 June, 2018.

[11] Bussemaker JH, Ciampa PD, Singh J, Fioriti M, Cabaleiro C, Wang Z, Peeters DMJ, Hansmann P, Della Vecchia P, and Mandorino M. Collaborative design of a business jet family using the AGILE 4.0 MBSE environment. *Proc 2022 AIAA AVIATION Forum*, Chicago, Illinois, 27 June – 1 July, 2022.

[12] Fioriti M, Cabaleiro C, Lefebvre T, Della Vecchia P, Mandorino M, Liscouet-Hanke S, Jeyaraj A, Donelli G, and

Jungo A. Multidisciplinary design of a more electric regional aircraft including certification constraints. *Proc 2022 AIAA AVIATION Forum*, Chicago, Illinois, 27 June – 1 July, 2022.

[13] Di Stasio M, Nicolosi F, Melone G and Cusati V. Conceptual design and technology sensitivity analysis of a fuel cell short-range aircraft. *Proc 2025 AIAA AVIATION Forum*, Las Vegas, Nevada, 21-25 July, 2025.

[14] Winnefeld C, Kadyk T, Bensmann B, Krewer U, and Hanke-Rauschenbach R. Modelling and designing cryogenic hydrogen tanks for future aircraft applications. *Energies*, Vol. 11, No. 1, 2018.

[15] Nicolosi F, Melone G, and Di Stasio M. Impact of thermal management system design on aircraft performance in hydrogen fuel cell powertrains. *Proc AIAA SciTech Forum 2026*, Orlando, Florida, 12-16 January, 2026.

[16] Marciello V, Cusati V, Nicolosi F, Saavedra-Rubio K, Pierrat E, Thonemann N, and Laurent A. Evaluating the economic landscape of hybrid-electric regional aircraft: A cost analysis across three time horizons. *Energy Conversion and Management*, Vol. 312, 2024.

[17] Cusati V, Di Stasio M, Lucci G, and Zhang Q. Evaluating hybrid-electric aircraft viability: The Ampaire Eco Caravan cost analysis. *Transportation Research Part D: Transport and Environment*, Vol. 144, 2025

[18] Gudmundsson S. *General aviation aircraft design: applied methods and procedures*. 2nd edition, Butterworth-Heinemann, 2022.

[19] The National Research Council (United States). *Improving the efficiency of engines for large nonfighter aircraft*. The National Academies Press, 2007.

[20] Marciello V, Di Stasio M, Ruocco M, Trifari V, Nicolosi F, Meindl M, Lemoine B, and Caliandro P. Design exploration for sustainable regional hybrid-electric aircraft: a study based on technology forecasts. *Aerospace*, Vol. 10, 2023.

[21] Roskam J. *Airplane design part VIII: airplane cost estimation*. DARcorporation, 2018.

[22] Wahler N, Ma Y, and Elham A. Conceptual design and aerostructural trade-offs in hydrogen-powered strut-braced wing aircraft: insights into dry and wet ultra-high aspect ratio wings. *Aerospace*, Vol. 12, 2025.